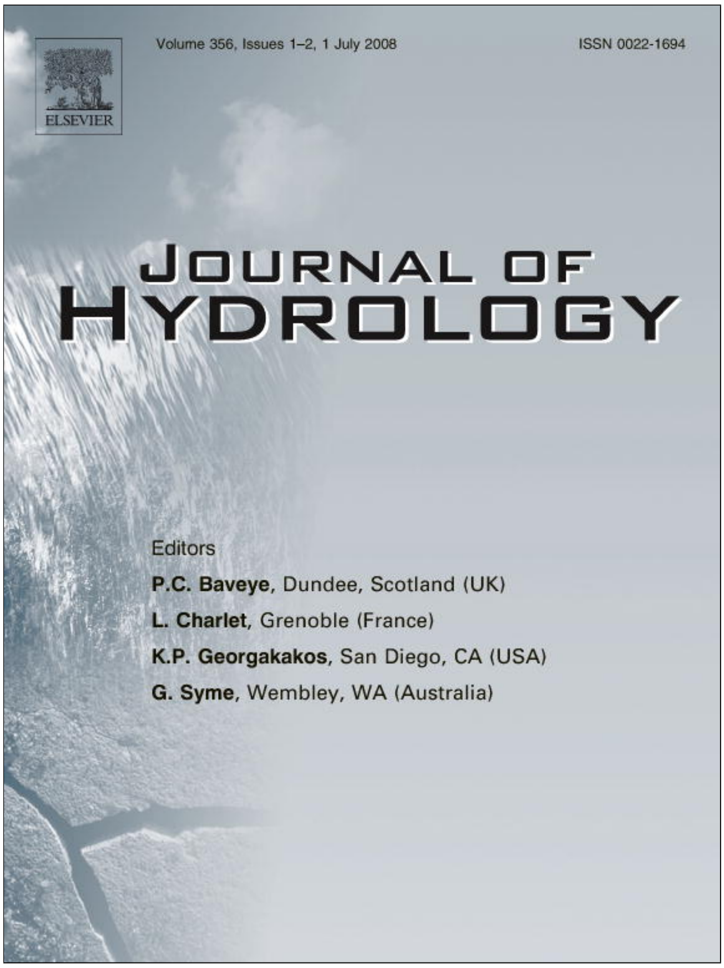
Volume 356, Issues 1–2, 1 July 2008
ISSN 0022-1694
ELSEVIER
JOURNAL OF
HYDROLOGY
Editors
P.C. Baveye, Dundee, Scotland (UK)
L. Charlet, Grenoble (France)
K.P. Georgakakos, San Diego, CA (USA)
G. Syme, Wembley, WA (Australia)

Journal of Hydrology (2008) **356**, 17–27

available at www.sciencedirect.com

ScienceDirect

journal homepage: www.elsevier.com/locate/jhydrol

Hydro-pedotransfer functions (HPTFs) for predicting annual percolation rate on a regional scale

G. Wessolek [a,*], W.H.M. Duijnisveld [b], S. Trinks [a]

[a] *Technical University Berlin, Department of Soil Protection, Salzufer 12, D-10587 Berlin, Germany*
[b] *Federal Institute for Geosciences and Natural Resources (BRG), Stilleweg 2, D-30655 Hannover, Germany*

Received 10 May 2007; received in revised form 21 January 2008; accepted 5 March 2008

KEYWORDS
Annual percolation rate;
Actual evapotranspiration;
Nonlinear regression equations;
Regional scale;
Regionalization;
Urban water components

Summary For predicting annual percolation rate at regional scales, we need robust methods that require only easily-available site information. This paper presents hydro-pedotransfer functions (HPTFs) that can be used to calculate annual percolation rates using such data for two land use categories: (i) plant-covered sites and (ii) urban sites with various degrees of surface sealing (i.e., % impervious surface). This paper explains the principle concepts and gives instructions for users.

A two-step procedure was used to derive HPTFs for plant-covered sites: (1) Step #1 involved scenario calculations of evapotranspiration and percolation rates for various soil, climate, groundwater, and crop conditions using a calibrated ''Soil-Water-Vegetation Model'' (aka ''SVAT''). (2) Step #2 used nonlinear multiple regression analysis of >50,000 annual SVAT simulations to develop easy-to-use HPTFs for cropland, grassland, coniferous forests, and deciduous forests. The new HPTFs require only these input data: (1) annual values of the FAO grass reference evapotranspiration and water supply during the vegetation growth period (these data summarize soil available water); (2) summer precipitation; and (3) capillary rise from the groundwater. Two HPTFs were developed for each land use type – one for site conditions with, and one without, water supply limitations. To handle urban areas, we also developed HPTFs for partly sealed areas, using data from lysimeter studies and inner-city percolation experiments. The HPTFs successfully calculated the mean annual percolation rate from soil within the ''Hydrological Atlas of Germany.'' HPTF results were validated by comparisons with gauge measured values taken in 106 catchments areas in Germany.

Introduction

Following Lin's (2003) ''Hydropedology'' approach, we try to bridge scales from ''pedons'' (= sites with specific

* Corresponding author. Tel.: +49 30 31473533; fax: +49 30 31423309.
E-mail addresses: gerd.wessolek@tu-berlin.de (G. Wessolek), duijnisveld@bgr.de (W.H.M. Duijnisveld).

0022-1694/$ - see front matter © 2008 Elsevier B.V. All rights reserved.
doi:10.1016/j.jhydrol.2008.03.007

Nomenclature

α	sealing index (percent sealed areas/100)	I	interflow (mm a^{-1})
β	infiltration coefficient (–)	P	annual precipitation at the soil surface (mm a^{-1})
β_s	summer infiltration coefficient (–)	P_s	precipitation during summer (April to September) (mm)
β_w	winter infiltration coefficient (–)	P_w	precipitation during winter (October to March) (mm)
γ	slope coefficient (–) expressing the influence of slope and sun exposure	$P*$	annual precipitation minus runoff (mm a^{-1})
ξ	slope (°)	$P*_s$	summer precipitation minus summer runoff of sealed sites (mm)
λ	sun exposure (°)	Q_a	actual annual amount of capillary rise (mm)
κ	coefficient to reduce E_0 for sealed surfaces (–)	Q_{cli}	upper limit of annual amount of capillary rise due to external conditions (climate, crop, soil) (mm)
Θ	soil water content (Vol%)	Q_{max}	maximum annual amount of capillary rise from the groundwater to the root zone, independent of climate conditions (mm)
h	pressure head (cm)	Q_{pot}	potential daily capillary rise from the groundwater into the effective root zone (mm d^{-1})
k	soil hydraulic conductivity (cm/d)	R	Total runoff depth (mm a^{-1})
z	vertical distance (cm)	R_0	surface runoff (mm A^{-1})
CWS	crop water supply, being the sum of W_a (Q_a and P_s)	$R_{0,s}$	surface runoff in the summer half-year (mm)
CWS_{crit}	critical water supply (mm)	R_{se}	annual surface runoff of sealed areas (mm a^{-1})
D_a	annual percolation out of the root zone (mm a^{-1})	T	length of the active period of capillary rise (d)
D_s	annual percolation of sealed surfaces (mm a^{-1})	W_a	plant available soil water within the root zone (mm)
D_u	annual percolation of urban areas (mm a^{-1})	ΔW	change of soil water storage in the root zone (mm)
E_a	annual actual evaporation (mm a^{-1})	Z_{GW}	depth groundwater table (cm)
E_0	annual potential evapotranspiration, represented by the FAO grass reference evapotranspiration (mm a^{-1})	Z_{root}	Depth of the root zone (cm)
E_{0r}	annual potential evapotranspiration corrected for slope and exposure (mm a^{-1})		
$E_{0,s}$	potential evapotranspiration during summer (April to September) (mm)		
ETI_a	annual actual evapotranspiration (mm a^{-1})		

characteristics) to landscapes by developing new algorithms which integrate information and approaches from soil, plant, and water sciences. To do this, here we introduce the descriptive new term ''hydro-pedotransfer- function'' (HPTF).

When a process analysis of water flow with high temporal and spatial resolution is needed, commonly one uses lysimeter data, soil-hydrological measurements, or simulation models (such as HYDRUS) (Moore et al., 1991). However, it is not feasible to carry out those approaches' intensive site measurements on a regional scale due to high costs or limitations of model input parameters (e.g., soil hydraulic functions; daily climate data).

Especially for land planners and geographers, one finds that often only annual values or long term means of the percolation rate are needed. That simple need is why empirical equations and nomograms have been developed in Germany to determine annual evapotranspiration and percolation rates at low temporal resolution (Renger and Strebel, 1980). To promote the broad use of such simplified methods in practice, we have developed empirical HPTFs based on real-world data, namely soil and climatic data for large areas.

The latest approach for Northern German sites (Renger and Wessolek, 1990) predicts the annual percolation rates under various land uses including coniferous forests, croplands and grasslands. However, their method could not be used everywhere in Germany, because they did not use the entire nation-wide spectrum of conditions in developing the model. Here, we seek to improve the ''Renger and Wessolek'' equations as follows, so as to expand the utility of the method and make it applicable throughout Germany:

- by including representative climatic regions of Germany covering the whole span of precipitation and potential evapotranspiration,
- by including the FAO's figures for grass reference evapotranspiration (E_0, see Allen et al., 1994). The FAO figures use a new, world wide uniform calculation method for potential evapotranspiration. This method should replace the Haude (1955) method (Dommermuth and Trampf, 1992).
- by including Richter's (1995) new corrections for precipitation observations (BMU, 2003), and
- by extending the model to urban areas, which are becoming more important in water management strategies, and therefore require extension to include sealed areas.

Principles and procedures to develop nonlinear HPTFs

Principles

Fig. 1 shows the soil water components as we used them. Annual water balance depends on precipitation (P), actual evapotranspiration (ETI_a), runoff (R_0), and percolation (D_a) from the root zone to the groundwater.

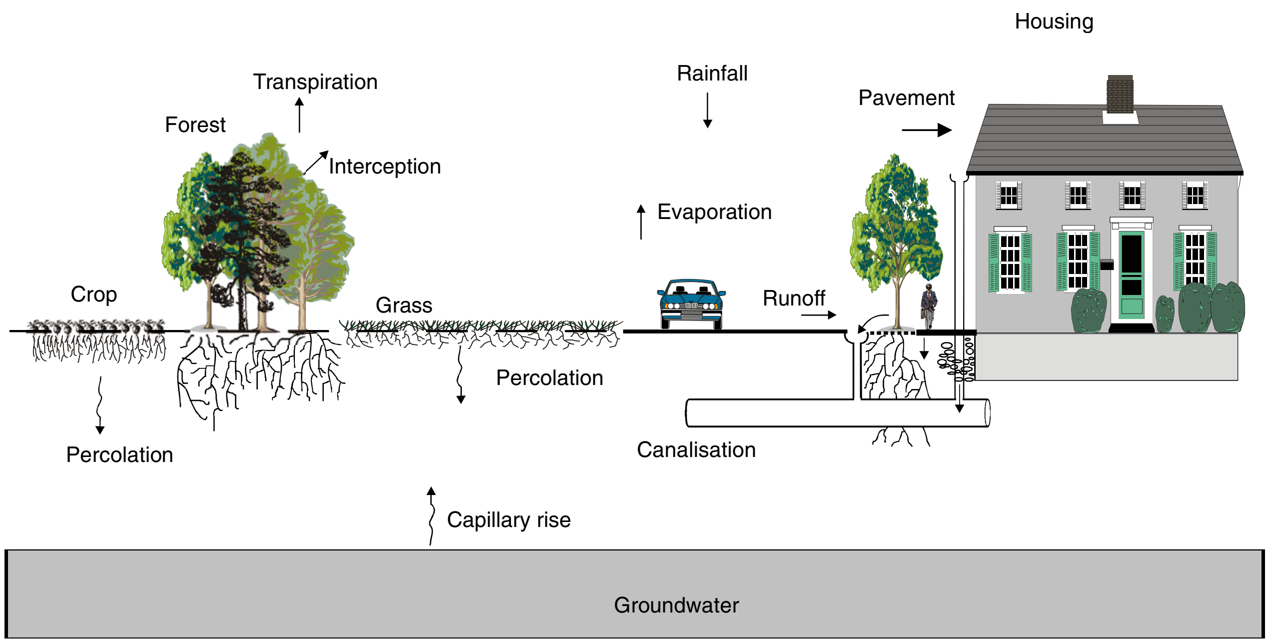

Figure 1 Schematic illustration of the components of soil water.

When plants are growing, ETI_a consists of interception, transpiration by plants, and evaporation from the bare soil. If depth to groundwater is shallow, capillary rise (Q_a) from the groundwater into the root zone can take place. In hilly regions, runoff (R_0) can occur, which may reduce actual evapotranspiration. Later is also depending on slope and sun exposure. If the soil surface is sealed with houses or pavement, part of the rainfall runs off or evaporates while the rest infiltrates through the soil-filled space between the sealing materials. The whole SVAT system is driven by two boundary conditions: energy from atmospheric conditions and water supply by rain, soil, and groundwater to enable evapotranspiration. Fig. 2 illustrates the basics of how we determined the new HPTFs.

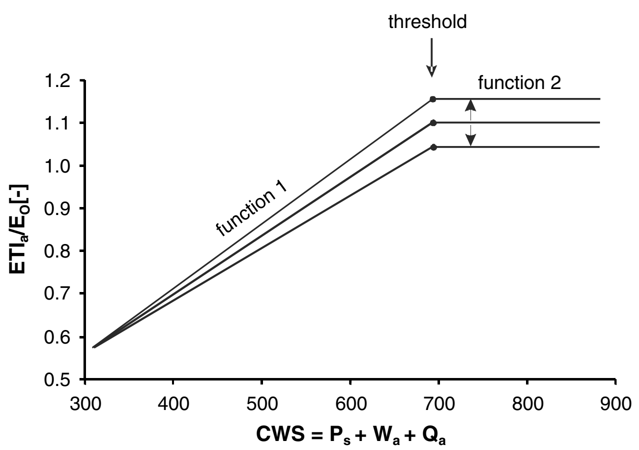

Figure 2 Basic principles for deriving the new HPTFs: the relation between crop water supply (CWS) and the ratio of actual to potential evapotranspiration (ETI_a/E_0).

As shown in Fig. 2, the ratio of actual (ETI_a) to potential evapotranspiration (E_0) is a function of the crop water supply (CWS) during the vegetation growth period (in Germany this is April–September). Our principle approach is based on the fact that actual evapotranspiration below a ''critical'' water supply threshold depends primarily on the availability of water (in Fig. 2 this threshold is about 700 mm).

In general, water supply can be expressed by these factors:

- cumulative precipitation during the growth period, minus surface runoff (P_s),
- plant available soil water in the effective root zone (W_a),
- capillary rise (Q_a) from groundwater into the root zone where shallow groundwater is present.

The ratio ETI_a/E_0 declines with decreasing CWS and is described by function 1. For optimal water supply conditions (above the threshold of the critical water supply), actual evapotranspiration (ETI_a) depends only on atmospheric conditions. Function 2 expresses these conditions depending only on the FAO grass reference evapotranspiration (E_0). Levels of functions 1 and 2 also depend on potential evapotranspiration (E_0), as shown in Fig. 2 by the upper and lower parts of functions 1 and 2. Below, we describe how to determine both functions as well as the critical water supply threshold for cropland, grassland, coniferous forest, and deciduous forest.

Procedures for deriving HPTFs

To develop the empirical nonlinear HPTFs, we correlate site-specific properties, climate, and land use factors, as explained in Table 1.

Step 1: Simulation model and calibration

Table 1 Procedure steps (1–4) for deriving HPTFs

Step 1: Simulation model and calibration
Calibration of a numerical simulation model using a wide variety of field measurements of soil moisture and water tension as a function of time and depth as well as actual evapotranspiration and percolation data from lysimeter measurements
Step 2: Scenarios with a SWAT-Model
Calculation of daily actual evapotranspiration and percolation rates for various land uses, climate stations, soils, and groundwater conditions
Step 3: Assumptions, and deriving HPTFs by multiple nonlinear regression analysis
Statistical evaluation of the model results and derivation of nonlinear regression equations (function 1 and function 2) that allow prediction of the annual percolation rate using only easily-available baseline data such as winter and summer precipitation, plant available soil water and potential evapotranspiration
Step 4: Validation of the HPTFs
Mean measured stream flow gauge data of 106 catchments were compared with results from the new HPTFs

A conventional soil–water–vegetation model (SVAT) was used to calculate daily rates of evapotranspiration and percolation (Wessolek et al., 2000), using these input parameters:

- daily climate data – precipitation, wind velocity, mean air temperature, mean air humidity, net radiation;
- soil hydraulic functions – soil water characteristics, unsaturated hydraulic conductivity, and depth to the groundwater table;
- plant data – degree of soil cover, root depth, plant height and plant resistance describing the water transport.

Evapotranspiration was calculated using a Penman–Monteith (1948,1988) approach as modified by Rijtema (1968). Soil hydraulic functions were determined using Plagge's (1991) instantaneous profile method. Model calibrations used either ETI_a measurements from field studies or lysimeter measurements (Wessolek et al., 2000). The measured field ETI_a values were based on soil moisture readings using TDR probes and hydraulic gradient predictions (via tensiometer). During the vegetation growth period, with zero flux plane conditions ($z = z_n$), ETI_a was calculated for discreet periods using field measurements of precipitation (P), hydraulic gradients and soil moisture change ($\Delta\Theta$) versus time (t) and depth (z), thusly –

$$ETI_a = P + \int_{t=t_1}^{t_n} \int_{z=0}^{z_n} \Delta\Theta(z,t)\,dz\,dt \qquad (1)$$

Table 2 gives an overview of the field investigations we used to calibrate the SVAT model, which will be applied in step 2 of Table 1.

In model calibration we varied rooting depth and plant resistances which describe (over time) the water transport from the soil into the roots and in the vegetation itself, to optimize simulated soil moisture and water tension so they will agree with measured data (Renger et al., 1986). Optimization of the plant-specific resistance was done to include (i) crop-related ETI_a differences (cropland < grassland < forest), (ii) soil-related ETI_a differences (sand < loam < silt), and (iii) groundwater-related ETI_a differences (deep groundwater < shallow groundwater conditions).

Step 2: Scenarios with the SVAT model

Combinations of site-specific conditions used in our numerical simulation scenarios included:

- four soil textures (fine sand, loamy sand, loam, silt) and plant available water;
- four land use types – cropland, grassland, pine forest, deciduous forest;
- six groundwater table depths (from 0.9 m to 2.8 m deep), and
- sixteen climate stations.

Altogether ~50,000 annual values of evapotranspiration were generated to create the data base from which the various HPTFs were derived statistically. Plant available soil

Table 2 Field measurements used for the calibration of the SVAT model

Land use	Location	Soil texture	Duration of the experiment
Coniferous and	Berlin (Grunewald, Spandau, Köpenick)	Sandy soil and silty sand	1984–2002
Deciduous forests	Hannover (Fuhrberger Feld)	Sandy soil	1976–1977
Grassland	Hannover (Fuhrberger Feld)	Sandy soil	1982
meadow	Berlin Berlin lysimeter	Sandy soil	1997
Cropland	Berlin	Loamy sand	1992–1995
	Bölkendorf	Loamy sand and sandy loam	1992–1996
	Adenstedt	Silty soils	1988–1990
	Hannover (Fuhrberger Feld)	Sandy soils	1976–1990
	Hannover (Ohlendorf)	Silt	1978–1983
	Darmstadt	Silty sand	1987–1988
	Göttingen	Silt	1977–1978
	Halle	Silt	1996–1999

water (pF 1.8 to pF 4.2) in the effective root zone (W_a) of the four soils varied from low (<70 mm) to high (>240 mm) (Table 3).

Table 3: Texture class, available soil water (mm), and field capacity (mm) in the effective root zone of the four soils used for the numerical simulation scenarios.

These soils represent a wide spectrum across the prevailing soil-hydrological site conditions for much of Germany, and are suitable for assessing the soil water balance.

The daily climatic data from sixteen German climate stations that were used to calculate evapotranspiration and percolation rates covered a 30-year period (1961–1991: Table 4). These 16 stations span typical climatic conditions in Germany, from low to high precipitation, and from humid and cool (hills, coast) to drier and warmer (continental). Mean annual precipitation varies between ~550 mm and >1300 mm. These data represent the precipitation at the soil surface according to Richter (1995). The climatic water balance (= precipitation minus potential evapotranspiration) in the summer half-year (April–September) is from <−130 mm to >440 mm.

Step 3: Assumptions and deriving HPTFs by multiple non-linear regression

Here we explain our simplifications of the general soil water balance, which were needed to develop practical, easy-to-use HPTFs.

We begin with

$$P = ETI_a + D_a + R_0 + I + \Delta W \tag{2}$$

wherein, P, precipitation; ETI_a, actual evapotranspiration; D_a, percolation rate; R_0, rurface Runoff; I, Interflow; ΔW, change of soil water storage in the root zone.

Applying Eq. (2) for annual water balances, ΔW becomes zero, because we calculated soil water balances between springs of the successive years with the soils being at field capacity (pF 1.8) in spring. We simulated only for plane

Table 3 Soil texture, plant available soil water (mm) and field capacity (mm) in the effective root depth of the four soils used for the numerical simulations

Texture				Arable land			Grassland			Forest		
Texture class	Sand %	Silt %	Clay %	W_a [a]	Fc [b]	We [c]	W_a [a]	Fc [b]	We [c]	W_a [a]	Fc [b]	We [c]
Fine sand	92	5	3	70	100	6	60	83	5	120	180	12
Loamy sand	75	20	5	110	185	7	95	160	6	170	310	12
Loam	58	32	10	170	260	8	150	230	7	250	370	12
Silt	3	86	11	240	360	10	215	324	9	310	432	12

[a] W_a = plant available soil water (pF 1.8–pF 4.2) in the effective root zone (mm).
[b] Fc = field capacity (pF 1.8) in the effective root zone (mm).
[c] We = depth of the effective root zone (dm).

Table 4 Averages of precipitation (corrected after Richter, 1995), FAO-grass reference evapotranspiration and summer water balance at various weather stations in Germany (Source: Deutscher Wetterdienst/German Weather Service)

Station	mP_s [mm]	mP_{win} [mm]	mP_a [mm. a^{-1}]	mE_0 [mm. a^{-1}]	$mE_{0,s}$ [mm]	$mCWB_{som}$ [mm]
Freiburg	610	412	1022	680	528	82
Würzburg	361	308	670	587	467	−106
Mannheim	428	310	738	619	495	−67
Stuttgart	460	272	732	598	469	−9
Coburg	440	387	827	509	419	21
München-Riem	685	423	1109	571	454	231
Kempten	838	576	1414	484	393	445
Bocholt	407	390	798	539	427	−20
Neumünster	455	435	890	499	411	44
Bremen	422	377	799	556	444	−22
Bad Hersfeld	418	379	797	501	410	8
Teterow	345	265	610	542	441	−96
Magdeburg	314	240	555	555	447	−133
Uelzen	384	308	691	495	408	−24
Braunlage	618	770	1388	441	367	251
Bocholt	371	351	722	539	427	−56

Where, mP_s, long term mean corrected precipitation in the summer half-year, April to September; mP_{win}, long term mean corrected precipitation in the winter half-year, October to March; mP_a, long term mean corrected yearly precipitation; mE_0, long term mean yearly FAO grass reference evapotranspiration; $mE_{0,s}$, long term mean FAO grass reference evapotranspiration in the summer half-year, April to September; $mCWB_{som}$, climatic water balance of the summer half-year, from April to September.

(i.e., horizontal) sites that have neither runoff nor interflow. These assumptions let us simplify Eq. (2) down to:

$$D_a = P - \mathrm{ETI}_a \quad (3)$$

Statistics

The ETI_a results of ~50,000 SVAT annual simulations were evaluated by means of nonlinear multiple regression analysis using the SPSS software package. Each annual ETI_a value was correlated with:

(i) potential FAO grass reference evapotranspiration (E_0), and
(ii) crop water supply (CWS).

As above, actual water supply (CWS) was defined by the sum of the plant available water in the root zone (W_a), the capillary rise from the groundwater to the root zone (Q_a) and the summer precipitation (P_s):

$$\mathrm{CWS} = W_a + Q_a + P_s \quad (4)$$

W_a is as a site-specific constant (see Table 3), but both Q_a and P_s vary from year to year. In our statistical evaluation, we first tested the principal hypothesis of Fig. 3 that ETI_a/E_0 raises until an optimal water supply is reached. Above this threshold of a critical water supply (CWS_{crit}), actual evapotranspiration depends only on atmospheric conditions.

We therefore calculated annually ETI_a/E_0 ratios for all soils and climate stations and plotted them against the water supply (CWS) as done for grassland in Fig. 3.

As expected, ETI_a increases until a land use specific CWS_{crit} is reached. Above this threshold, ETI_a is limited only by the potential evapotranspiration level (E_0). To distinguish between site conditions with and without a sufficient water supply, two HPTFs were derived for land use type.

Step 4: Validation of the HPTF

To validate the HPTFs, we compared long term mean annual values of rainfall minus calculated actual evapotranspiration ETI_a from 106 German catchment areas with the long term mean annual total runoff as measured by stream flow gauges. In hilly regions, slope surface runoff (R_0) was also taken into account ($D_a + R_0$) using the curve number approach (Hope and Schulze, 1982), details are in Jankiewicz et al., 2005. The catchments differed in size, land use, soil properties, and geomorphologic and climatic conditions (Fig. 4).

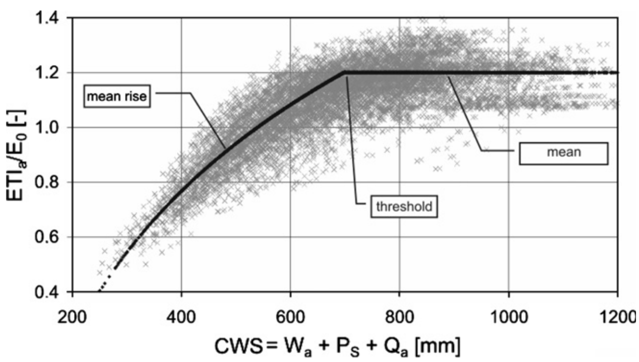

Figure 3 Relation between ETI_a/E_0 and crop water supply (CWS) for grasslands.

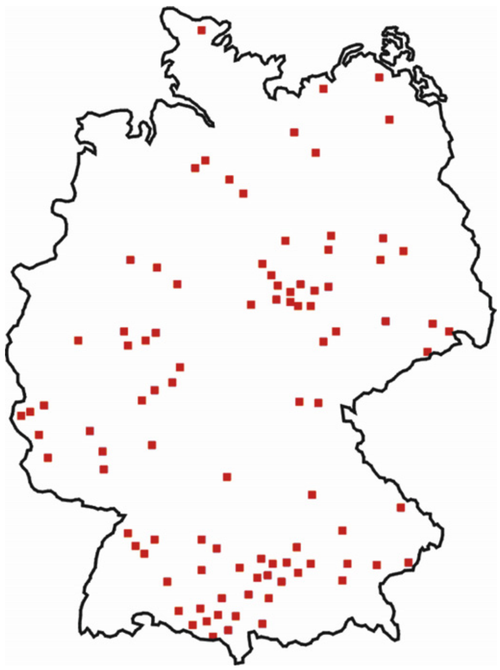

Figure 4 Catchment areas in Germany used to validate the regression water balances.

Results and discussion

HPTFs for croplands, grasslands, coniferous and deciduous forests

We used SPSS to calculate nonlinear regressions for all soils, types of land use, climate stations and groundwater table conditions. For the four land uses (cropland, grassland, coniferous and deciduous forests) and water supply conditions, a total of eight regression equations were determined to estimate annual percolation rates. The HPTFs so generated are listed in Table 5.

To distinguish between (a) site conditions that do not have a sufficient water supply to enable potential evapotranspiration (=function 1, Fig. 2) and (b) those with a sufficient water supply to do so (=function 2, Fig. 2), two HPTFs for each crop type were derived by introducing a threshold of a critical water supply. In Germany, the average critical water supply (CWS_{crit}) to guarantee a good water supply varies: it is about 700 mm for cropland and grassland, and 750 mm for forest. These are slightly greater than potential evapotranspiration and guarantee optimal crop development.

HPTF for urban areas

If one wishes to calculate water components in urban areas, a sealing index α (=% sealed area) must first be obtained either by prediction (using a model), or more directly by using mapping or remote sensing (Bogena et al., 2004). The annual percolation rate of urban sites (D_u) including percolation from both sealed (D_s) and unsealed areas (D_a) is expressed thus by:

$$D_u = \alpha D_s + (1 - \alpha) D_a \quad (5)$$

Table 5 HPTFs to predict the annual percolation rate (D_a) for arable lands, grasslands, coniferous forests, and deciduous forests

Arable land

if $CWS_{crit} > 650$ mm then:

$D_a = P_a - 1.05\ E_0\ (0.685 \log(1/E_0) + 2.865)$

if $CWS_{crit} < 650$ mm then:

$D_a = P_a - E_0\ (1.45 \log(W_a + Q_a + P_S) - 3.08)\ (0.685 \log(1/E_0) + 2.865)$

Grassland

if $CWS_{crit} > 650$ mm then:

$D_a = P_a - 1.2\ E_0\ (0.53 \log(1/E_0) + 2.43)$

if $CWS_{crit} < 650$ mm then:

$D_a = P_a - E_0\ (1.79 \log(W_a + Q_a + P_S) - 3.89)\ (0.53 \log(1/E_0) + 2.43)$

Forest

if $CWS_{crit} > 700$ mm then:

Coniferous $D_a = P_a - 1.3\ E_0\ (0.865 \log(1/E_0) + 3.36)$

Deciduous $D_a = P_a - 1.17\ E_0\ (0.865 \log(1/E_0) + 3.36)$

if $CWS_{crit} < 700$ mm then:

Coniferous $D_a = P_a - E_0\ \lfloor 1.68 \log(W_a + Q_g + P_S) - 3.53 \rfloor (0.865 \log(1/E_0) + 3.36)$

Deciduous $D_a = P_a - 0.90 \cdot E_0\ (1.68 \log(W_a + Q_a + P_S) - 3.53)\ (0.865 \log(1/E_0) + 3.36)$

D_a can be calculated using the equations of Table 5. However, D_s considers the amount of surface runoff (R_{se}) and actual evapotranspiration (ETI_a) from the sealed surface, and is expressed as:

$$D_s = P - (R_{se} + ETI_a) \quad (6)$$

Lysimeter studies and infiltration measurements from various urban areas show that R_{se} varies widely, and depends on the space between pavement materials, rainfall intensity, and age of the pavement. During aging of the pavement, dust input reduces infiltration and increases runoff (Breuste, 1996; Flöter, 2006; Wessolek and Facklam, 1997; Nehls et al., 2006). For predicting annual values, we suggest using β-infiltration coefficients (Table 6) to express both (i) the runoff (R_{os}) leaving the sealed surface, and (ii) the amount of rainfall that infiltrates (P_{inf}) into the seam material or through fissures in the soil. Because of different rainfall types and conditions during the year, we also suggest distinguishing between runoff induced by summer precipitation (P_s) and winter precipitation (P_w) when calculating total annual runoff of partly sealed surfaces (R_{se}). Thus, we distinguish between β-coefficients for summer (with higher rainfall intensities) and winter seasons (Table 6).

The infiltration coefficient β(0–1) express the ability of the partly sealed surface to infiltrate rainfall through seam material and fissures. With increasing β, R_{se} becomes smaller:

$$R_{se} = P_s^*(1 - \beta_s) + P_w^*(1 - \beta_w) \quad (7)$$

The β-coefficients were obtained from lysimeter experiments (Flöter, 2006; Wessolek and Facklam, 1997). Using the β-coefficients of Table 6, one can easily estimate the net precipitation (P^*) which is infiltrating into the soil of partly sealed sites.

$$P^* = P - R_{se} \quad (8)$$

The annual actual evaporation (ETI_a) of partly sealed areas can be calculated using E_0 and a reduction coefficient (κ). That coefficient κ can be calculated by Eq. (10) (below), where net summer precipitation is defined as $P_s^*(= P_s^*\beta_s)$. The value 0.6 is a calibration factor, as measured against ETI_a using the above-mentioned Lysimeter data. The sealing materials themselves have a very low water storage capacity (Wessolek and Facklam, 1997), so we neglected it in calculating κ.

$$ETI_a = \kappa * E_0 \quad (9)$$

$$\text{with } \kappa = \left(\frac{\log(0.6 * \beta_S * P_s^*)}{\log(E_0)}\right)^4 \quad (10)$$

Fig. 5 shows the calibration result of Eq. (9) using Lysimeter measurements taken in Berlin and Hamburg, with different sealing materials (i.e., different β-coefficients). Though the lysimeter measurements are quite scattered, ETI_a can be predicted with an accuracy of about ±50 mm using site-specific β-coefficients.

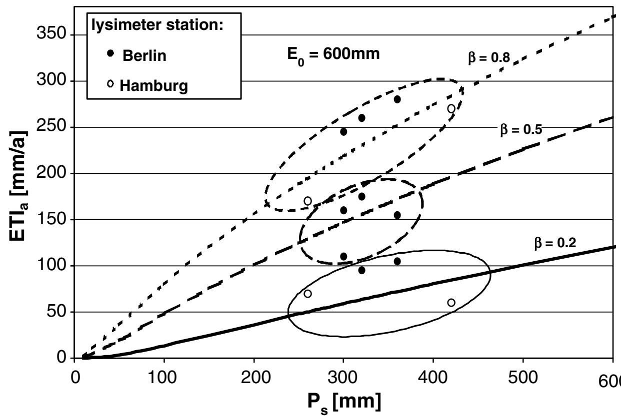

Figure 5 Actual evapotranspiration of sealed sites predicted with Eq. (9) compared with lysimeter studies from Berlin (Wessolek and Facklam, 1997) and Hamburg (Flöter, 2006).

Table 6 Summer (β_s) and winter (β_w) infiltration coefficients for different sealing materials

Degree of surface sealing	β_s	β_w	Examples
Class I (low: <10%)	0.90	0.95	Open concrete stones filled with grass vegetation
Class II (medium: 10–50%)	0.80	0.85	Mosaic cobble stones
Class III (high: 90–50%)	0.55	0.60	Concrete pavement
Class IV (severe: >90 %)	0.20	0.25	Asphalt street, roof

Instructions for using the new HPTFs

To use the new HPTFs efficiently, one needs to calculate (i) plant available water (W_a) and (ii) capillary rise (Q_a). (iii) Also, in hilly regions the influence of slope on actual evapotranspiration and surface runoff should be considered.

(i) Plant available soil water (W_a)

To estimate plant available soil water, one can use soil physical field and laboratory measurements. If such data are not available, pedotransfer functions (PTFs) can be used to predict soil water retention (Vereecken et al., 1989; Wösten et al., 1999; Zacharias and Wessolek, 2007). Other usable data are often available through the national soil survey.

For Germany, across all soil textures and land uses, W_a lies at 50–300 mm, and effective root depth can be 5 to >12 dm (Soil Classification System KA5 Ad-Hoc AG Boden, 2005). Lower values of W_a are typical for sandy and heavy clay soils or for soils with a small weathered root zone above hard rocks.

(ii) Capillary rise (Q_a)

Since the actual, average capillary rise from groundwater (Q_a) depends on both soil hydraulic functions and climate (potential evapotranspiration), both soil- and climate-specific limitations of total capillary rise should be considered for the HPTFs in Table 5.

First one needs to calculate soil-specific capillary rise rates: we call them ''potential capillary rise rates'' (Q_{pot}) because they express the potential daily upward flow rates *without* climatic limitation. Steady-state capillary flow rates can be predicted easily by the Darcy equation:

$$Q_{pot} = -k\left(\frac{dh}{dz} + 1\right) \quad (11)$$

wherein, Q_{pot}, potential capillary rise rate (cm/d); h, pressure head (cm); z, vertical distance (cm); k, soil hydraulic conductivity (cm/d).

Integrating of Eq. (11) yields

$$\int_{z1}^{z2} dz = \int_{h1}^{h2} \frac{-1}{1 + Q_{pot}} dh. \quad (12)$$

Starting at the groundwater table where $h = 0$, one can calculate pressure head profiles with depth, i.e. $h(z)$ for various flux values (Q_{pot}).

Many authors (e.g., Bloemen, 1983; Brandyk and Wesseling, 1985; Renger and Strebel, 1980) calculated them by solving Eq. (12) numerically for various steady-state pressure heads and distances between the groundwater table and the bottom of the effective root zone. Fig. 6 shows such capillary rise rates for the soils, as we used them in our numerical simulations.

Next, we need the land use specific time (*T in days*) during which we can expect an active capillary rise. In Germany, this period varies between 25 days (summer cereals on soils with a low PAW and low values of Q_{pot}) up to 120 days (grasslands and forests with shallow groundwater tables). Detailed

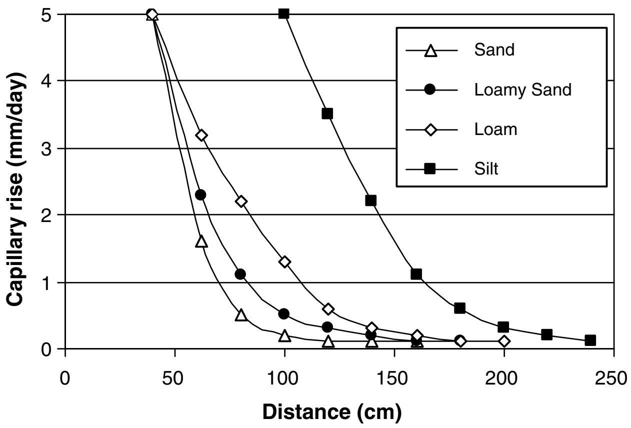

Figure 6 Potential capillary rise rates (Q_{pot}) for the soils used in our numerical studies, as a function of the distance between groundwater table and the lower boundary of the effective root zone.

information is in Ad-Hoc AG Boden (2005). Hence, the maximum annual capillary rise of groundwater (Q_{max}) to the root zone is given by

$$Q_{max} = Q_{pot} \cdot T \quad (13)$$

Finally, we consider the upper limit of capillary rise depending solely on climatic conditions. We call this the ''climate-controlled annual capillary rise'' (Q_{cli}), and it is calculated using a site-specific equation:

$$Q_{cli} = g \cdot E_{0,S} - (P_s + 0.5\,W_a) \quad (14)$$

The empirical coefficient g is 1.05 for cropland, 1.2 for grassland and 1.3 for both coniferous and deciduous forests. This is an expression of methodological differences in the calculation of the potential evapotranspiration in the SVAT model (done with a modified Penman–Monteith-approach) and the FAO grass reference evapotranspiration (as used to generate HPTFs). The coefficient 0.5 in Eq. (14) results from field measurements on sites with a shallow groundwater table in which capillary rise into the root zone started when soil water was <50% W_a (Renger and Strebel, 1980).

$E_{0,S}$ in Eq. (15) can be easily calculated by a simple linear regression equation relating the FAO grass reference evapotranspiration of the summer half-year (from April to 30 September: $E_{0,S}$) to E_0 of the entire year. This has been predicted for the locations indicated in Table 3 for 1961–1990. A linear regression analysis between E_0 and $E_{0,S}$ shows a good relationship (Fig. 7). The equation for German climate conditions is:

$$E_{0,S} = 0.72E_0 + 48 \quad (r^2 = 0.9451) \quad (15)$$

This strong correlation is to be expected, since the variables are not independent. However, because the relationship is being used not as an explanation but as a predictor only, the plot is useful and informative. Among other things, it shows that potential summer evapotranspiration is about 75% of the annual potential evapotranspiration, thus allowing people who need summer half-year values (which are often not available) to estimate them from available annual values (which are usually available).

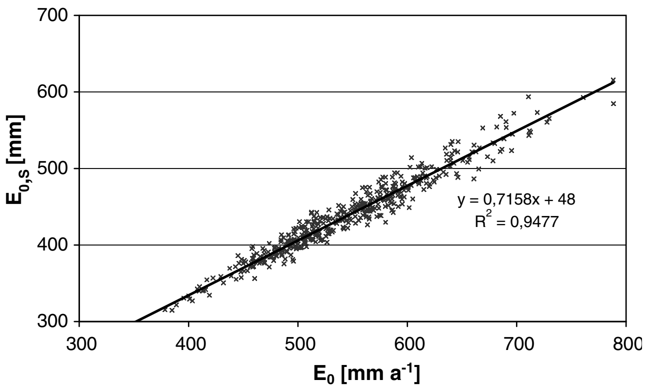

Figure 7 Grass reference evapotranspiration of the summer half-years ($E_{0,s}$) plotted against to values of the entire year (E_0).

To make a realistic assessment of the actual amount of annual capillary rise (Q_a) needed in the HPTF (Table 5), three conditions may be distinguished:

- if $Q_{cli} < 0$ then $Q_a = 0$
- if $Q_{max} > Q_{cli}$ then $Q_a = Q_{cli}$ (16)
- if $Q_{max} \leqslant Q_{cli}$ then $Q_a = Q_{max}$

(iii) Slope, sun exposure and surface runoff

In hilly regions, slope (ξ, °) and sun exposure (λ, °) should be considered in calculations of potential evapotranspiration. We parameterised a complex approach (Junghans, 1969) to derive a relatively simple γ -coefficient that increases or reduces E_{0r} as a function of exposure and slope:

$$E_{0r} = \gamma * E_0 \quad \text{wherein}$$
$$\gamma = 0.0023 * \lambda + 0.015 * \lambda * \sin(\xi - 90^\circ) + 1 \qquad (17)$$

Here, E_{0r}, annual potential FAO grass reference evapotranspiration for sites with slope; ξ, slope (°); λ, exposure (0° = north, 90° = east, 180° = south, 270° = west).

Fig. 8 demonstrates how γ significantly reduces E_0 for northern slopes and increases E_0 for southern slopes, while the corrections for eastern- and western-oriented slopes are more moderate (±10%). E_{0s} should be used for the HPTFs in Table 5 for hilly regions.

In croplands where surface runoff (R_0) may occur, part of the summer and annual rainfall will not be available for evapotranspiration. To include this in calculations of actual evapotranspiration, we suggest the following. Surface runoff can be calculated, for example, by using a modified curve number method (USDA-SCS, 1972; DVWK, 1984; Grove et al., 1998). If data for summer surface runoff $R_{0,s}$ are available, they can be directly used to reduce the summer rainfall (P_s) in the HPTFs of Table 5. If such information is not available, we suggest reducing summer rainfall by half of the yearly surface runoff R_0 when one calculates actual evapotranspiration by using the HPTFs in Table 5. Also, the equation to calculate the annual percolation rate D_a has to be corrected for surface runoff:

$$D_a = P_a - R_0 - \text{ETI}_a \qquad (18)$$

As can been seen from the above descriptions of how to actually use the new HPTFs, soil water balances can be predicted for various site conditions using easily-available information about soil, land use, groundwater, slope, and climate conditions.

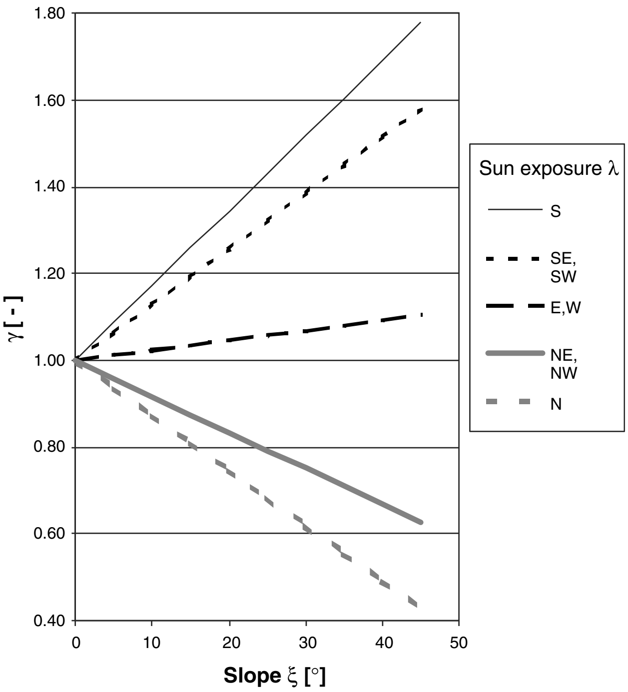

Figure 8 Influence of slope and sun exposure on E_0 expressed by Eq. (17).

Validation of the HPTFs

To verify the new HPTFs, the predicted total runoff depth R (mean rate of percolation D_a plus surface runoff R_0) was compared with the runoff measured by stream flow gauges in 106 catchment areas of different sizes, land uses, soil properties, geomorphological conditions, and climates. Regression analysis shows a good correlation between the

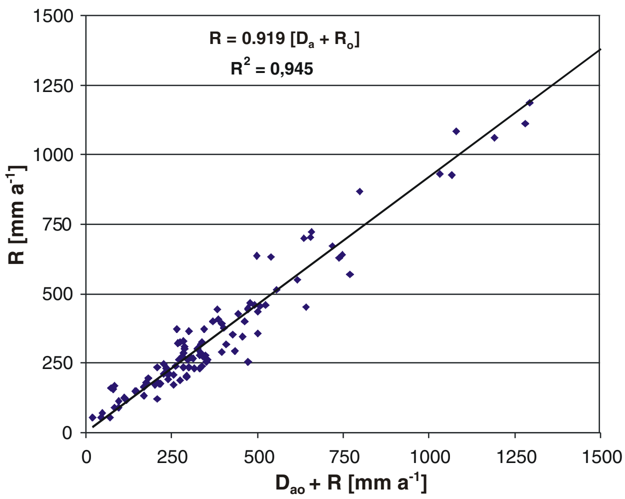

Figure 9 Mean measured annual runoff depth R versus predicted runoff depth ($D_a + R_0$) for 106 catchment areas in Germany.

measured and calculated values (Fig. 9), with the calculated values averaging only about 8% higher than measured.

Differences between measured and calculated runoffs might be caused by anthropogenic influences (e.g., extraction of groundwater), which were not considered in our predictions. Glugla et al. (2003) used another method (BAGLUVA-Method) to compute the total runoff depth *R* of the same test catchments areas. Their predicted total runoff depth was also higher than the measured values, and by about the same amount as our estimates (Jankiewicz et al., 2005).

Conclusion

We developed new HPTFs to use in predicting soil percolation rates across all of Germany. The HPTFs take into account soil conditions, vegetation, and land uses. They can also easily include other important factors such as slope, degree of soil sealing, and sun exposure. Actual real-world use of the new HPTFs requires only easy-to-obtain input data.

This is the first study to include sealed sites from urban areas. Such areas will require more attention in future research projects because urban sprawl and development change pedo-hydrological processes, leading to frequent flooding and draught.

To further improve the new method, we will need better estimates of the total capillary rise from groundwater into the root zone, because today's method for those data is relatively general and does not yet take into account the differences between climatic regions. We need also to understand the current over-prediction of total runoff by both our new HPTFs and other models. Studies of the amount and distribution of surface runoff as a function of time could help us produce a more accurate calculation of reduced evapotranspiration.

Acknowledgement

Thanks to Dr. Eric Shulenberger, University of Washington, (Multidisciplinary Research and Proposal Development) for his very helpful suggestions improving the manuscript, his comments and his linguistic support. We thank Michael Facklam for his technical support and Helena Schmieschek for data processing, preparing drawings, and tables. The authors are grateful to the German Research Foundation (DFG) and the BGR-Hannover for funding us.

References

Ad-hoc-AG Boden, 2005. Bodenkundliche Kartieranleitung KA5. Schweizerbart, Stuttgart, 438 p.

Allen, R.G., Smith, M., Perrier, A., Pereira, L.S., 1994. An update of reference evapotranspiration. ICID Bulletin 43 (2), 1–34.

Bloemen, G.W., 1983. Calculation of hydraulic conductivities and steady state capillary rise in peat soils from bulk density and solid matter volume. Journal of Plant Nutritional Soil Science 146 (4), 460–473.

BMU (Bundesministerium für Umwelt, Naturschutz und Reaktorsicherheit, Ed.), 1998, 2001, 2003. Hydrologischer Atlas von Deutschland. 1. Lieferung (1998), 2. Lieferung (2001) und 3. Lieferung (2003). Bonn.

Bogena, H., Herbst, M., Kunkel, R., Vereecken, H., Wendland, F., 2004. Skalenabhängige Modellierung des Wasserhaushalts im Flusseinzugsgebiet der Rur. Report of the Forschungszentrum Jülich, 21 pp. (in German).

Brandyk, K., Wesseling, J.G., 1985. Steady state capillary rise in some soil profiles. Journal of Plant Nutritional Soil Science 148, 54–64.

Breuste, J., Keidel, T., Meinel, G., Münchow, B., Netzband, M., Schramm, M., 1996. On analyzing and predicting surface sealing. UFZ-Leipzig report of ecological studies No. 7, 230 p. (in German, ISSN 0948-9452).

Dommermuth, H., Trampf, W., 1992. Die Verdunstung in der Bundesrepublik Deutschland Zeitraum 1951–1980. Deutscher Wetterdienst, Offenbach, 13 Karten, 10 p.

DVWK, 1984. Arbeitsanleitung zur Anwendung von Niederschlags-Abfluss-Modellen in kleinen Einzugsgebieten, Regel 113.

Flöter, O., 2006. Wasserhaushalt gepflasterter Strassen und Gehwege. Lysimeterversuche an drei Aufbauten unter praxisnahen Bedingungen unter Hamburger Klima. Dissertation, Hamburger Bodenkundliche Arbeiten, ISSN: 0724-6382, 329 p.

Glugla, G., Jjankiewicz, P., Rachomow, C., Lojek, K., Richter, K., Fürtig, G., Krahe, P., 2003. Wasserhaushaltsverfahren zur Berechnung vieljähriger Mittelwerte der tatsächlichen Verdunstung und des Gesamtabflusses. Bundesanstalt für Gewässerkunde, Koblenz, Berlin, Report No. 1342, 184 p.

Grove, M., Harbor, J., Engle, B., 1998. Composite vs. distributed curve numbers: Effects on estimates of storm runoff depths: Journal of the American Water Resources Association, 34, 5 p.

Haude, W., 1955. Zur Bestimmung der Verdunstung auf möglichst einfache Weise. In: DVWK, 1996. Ermittlung der Verdunstung von Land- und Wasserflächen. Merkblätter zur Wasserwirtschaft No. 238, 135 p.

Hope, A.S., Schulze, R.E., 1982. Improved estimates of storm flow volumes using the SCS curve number method. In: Singh, V.P. (Ed.), Rainfall-runoff Relationships. Water Resources Publications, Littleton, pp. 419–431.

Jankiewicz, P., Neumann, J., Duijnisveld, W.H.M., Wessolek, G., Wycisk, P., Hennings, V., 2005. Abflusshöhe, Sickerwasserrate, Grundwasserneubildung. Drei Themen im Hydrolo-gischen Atlas von Deutschland. Z. Hydrologie und Wasserwirtschaft, 49, 1, 2–13.

Junghans, H., 1969. Sonnenscheindauer und Strahlungsempfang geneigter Flächen. Abhandlungen des Meteorologischen Dienstes der Deutschen Demokratischen Republik, No. 85, 11, 106 p.

Lin, H.S., 2003. Hydropedology: bridging disciplines, scales, and data. Vadose Zone Journal 2, 1–11.

Monteith, J.L., 1988. Does transpiration limit the growth of vegetation or vice versa? Journal of Hydrology 100, 57–68.

Moore, I.D., Grayson, R.B., Ladson, A.R., 1991. Digital terrain modelling: A review of hydrological, geomorphological and biological applications. Hydrology Processes 5, 3–30.

Nehls, T., Jozefaciuk, G., Sokolowska, Z., Hajnos, M., Wessolek, G., 2006. Pore-system characteristics of pavement seam materials of urban sites. Journal of Plant Nuitritional Soil Science 169, 16–24.

Penman, H.L., 1948. Natural evaporation from open water, bare soil and grass. Proceedings of Royal Meteorological Society of America 193, 120–145.

Plagge, R., 1991. Bestimmung der ungesättigten hydraulischen Leitfähigkeit im Boden. Thesis, Bodenökologie und Bodengenese, 3, Dissertation. Institute of Ecology, Technical University Berlin, 152 p.

Renger, M., Strebel, O., 1980. Jährliche Grundwasserneubildung in Abhängigkeit von Bodennutzung und Bodeneigenschaften. Wasser und Boden 32 (8), 362–366.

Renger, M., Wessolek, G., 1990. Auswirkungen von Grundwasserabsenkungen und Nutzungsänderungen auf die Grundwasserneubildung. Mitt. Inst. für Wasserwesen, Bundeswehr Hochschule München, Vol. 38 B, 295—305.

Renger, M., Strebel, O., Wessolek, G., Duynisveld, W., 1986. Evapotranspiration and groundwater recharge — a case study for different climate, crop patterns, soil properties and groundwater depth conditions. Journal of Plant Nutritional Soil Science, 371—382.

Rijtema, P.E., 1968. On the relation between transpiration, soil physical properties and crop production as a basis for water supply plans. Techn. Bulletin 58 Inst. for Land and Water Management Res. Wageningen, 134 p.

Richter, D., 1995. Ergebnisse methodischer Untersuchungen zur Korrektur des systematischen Messfehlers des Hellmann-Niederschlagsmessers. Berichte des Deutschen Wetterdienstes Nr. 194, Offenbach, 178 p.

USDA-SCS, 1972. National Engineering Handbook. Section 4. Hydrology.

Vereecken, H., Feyen, J., Maes, J., Darius, P., 1989. Estimating the soil moisture retention characteristic from texture, bulk density and carbon content. Soil Science 148, 389—403.

Wessolek, G., Gross, J., Hammel, K., 2000. Water and bromide transport in a heterogeneous glacial sand. Journal of Plant Nutritional Soil Science 1 (163), 13—20.

Wessolek, G., Facklam, M., 1997. Site conditions and water components of sealed areas. Journal Plant Nutritional Soil Science 160, 41—46 (in German).

Wösten, J.H.M., Lilly, A., Nemes, A., Le Bas, C., 1999. Development and use of a database of hydraulic properties of European soils. Geoderma 90, 169—185.

Zacharias, S., Wessolek, G., 2007. Excluding organic matter content from pedotransfer predictors of soil water retention. Soil Science Society of American Journal 71, 43—50.